

Acoustic impedance measurement with grazing flow

Cécile Malmay and Serge Carbonne,
*EADS Airbus SA, Laboratoire d'Acoustique et Vibration,
B.P. M6332, 31060 Toulouse, France,*
Yves Aurégan and Vincent Pagneux,
*Lab. Acoustique Université du Maine, UMR CNRS 6613,
Université du Maine, 72085 Le Mans, France*

Lasting increasing of air traffic will only be feasible if noise pollution near airports, due to aircraft flyover, is significantly reduced. Among acoustic emissions from the aircraft, engine noise, and particularly fan noise, is a preponderant source. In order to reduce this noise, the nacelle is lined with absorbing materials made of a thin layer (such as perforated plate) bounded to partitioned air cavities. These treatments are submitted to high sound pressure levels (up to 160 dB) and high flow Mach numbers (up to 0.7). The key design parameter is the acoustic impedance of treatment panels, which depends on sound frequency, sound pressure level and flow Mach number. Acoustic impedance properties are mainly quantified by semi or totally empirical formulas, which depend on the experimental set-up used and are specific for each type of tested layer. Therefore, EADS acoustic laboratory has got an experimental set-up measuring acoustic impedance of liners used on Airbus aircrafts. This paper presents some of existing models for perforated plates impedance, describes the experimental set-up used and shows some results that are compared with empirical models from literature. It is shown that models valid up to Mach 0.2 seem to be valid up to Mach 0.6.

Nomenclature

c_0	Speed of sound in fluid at rest, m.s^{-1}
d	Orifice diameter, m
e	Resistive layer thickness, m
f	Frequency, Hz
k	Wave number, m^{-1}
M	Mean flow Mach number
L	Cavity depth, m
r	Resistive layer normalized resistance
v_0	Incident acoustic velocity on one orifice, m.s^{-1}
v	Incident acoustic velocity on the plate, m.s^{-1}
v^*	Friction velocity of the flow, m.s^{-1}
y	Duct section coordinate, m
z	Resistive layer normalized specific acoustic impedance
z_t	Total normalized specific acoustic impedance (resistive layer + cavity)
χ	Resistive layer normalized reactance
ω	Pulsation, rad.s^{-1}
ρ_0	Fluid density, kg.m^{-3}
σ	Perforated plate porosity : $\sigma = \frac{nS}{S}$, where n is the number of holes in the plate, s is one hole area and S is total area

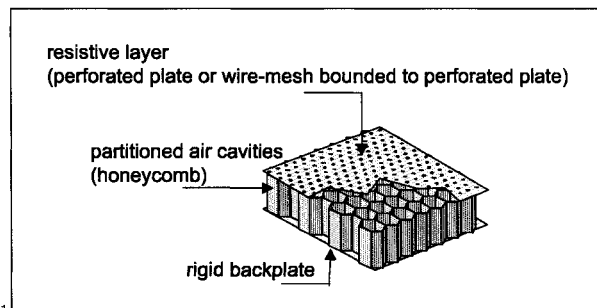


Fig. 1 Acoustic treatment used in turbojet engines

Introduction

Noise sources in a turbofan engine come from the turbofan, compressor, turbine and combustor. The turbofan produces a pure tone sound called "Blade Passage Frequency", and its harmonics. The BPF depends on the flight RPM, and is comprised between 800 and 8000 Hz. The acoustic levels can reach 160 dB (re 20 μPa).

Turbofan noise is attenuated by the acoustic treatment which lines the internal part of the nacelle. The treatments consist of a sandwich construction with a rigid backplate, a cellular separator such as honeycomb and a thin layer (perforated plate or wire-mesh), called resistive layer (see figure 1). They are submitted to high sound pressure levels and high flow velocities (up to 240 m/s).

In order to optimize these acoustic treatments, modelling of the propagation of acoustic waves in ducts and their radiation in the farfield is needed. EADS Airbus uses equally analytical approaches and numerical methods to describe the propagation in lined ducts with axial flow and the radiation of acoustic waves in farfield¹.

In the model, we need to know boundary conditions at the treated wall (see for example ref.² for boundary conditions with grazing flow at a lined wall). These conditions depend on acoustic properties of the absorbing material. At the treatment surface, pressure field is perturbed by (thin plate) local phenomena, which are not negligible. For instance, in the case of a perforated plate, non-linear phenomena are observed around plate orifices, due to high values of acoustic velocity. Moreover, there is an interaction between acoustic field and tangential air flow at the treatment surface. Present state of analytical and numerical codes do not permit to model these interactions directly in the sound pressure calculation. It is thus necessary to have a parameter which characterizes wall conditions, not only as a function of treatment geometry, but also as a function of external environment (sound frequency, acoustic velocity amplitude and flow characteristics). An “equivalent” boundary condition is then required to take into account all these effects.

The key parameter to quantify these effects is the acoustic impedance at the surface of the treatment. The normal specific normalized acoustic impedance will be used here, i.e. :

$$z_t = \frac{1}{\rho_0 c_0} \frac{p}{\vec{v} \cdot \vec{n}}, \tag{1}$$

where :

p is the acoustic pressure at a point of the surface of the liner,

\vec{v} is the acoustic velocity at the same point,

\vec{n} is the normal to the surface of the liner,

c_0 is the speed of sound in air,

ρ_0 is the air density.

The thickness of the plate being much lower than acoustic wavelength, continuity of normal acoustic velocity at each side of the layer can be assumed. An impedance “jump” can therefore be defined³, called “layer impedance” z :

$$z = \frac{1}{\rho_0 c_0} \frac{p - p_1}{\vec{v} \cdot \vec{n}}, \tag{2}$$

where $(p - p_1)$ is the pressure drop across the layer (see figure 2).

In this paper z will be written :

$$z = r + j\chi, \tag{3}$$

where r is the normalized specific acoustic resistance of the layer and χ is the normalized specific acoustic reactance.

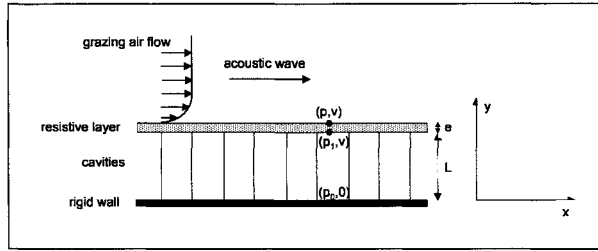


Fig. 2 Acoustic treatment (cut view) and aeroacoustic characteristics

Total impedance z_t is then the sum of layer impedance and cavity impedance, given by :

$$z_t = z - j\cot(kL), \tag{4}$$

where :

k is the acoustic wave number : $k = \frac{\omega}{c_0}$,

L is the cavity depth.

According to the above considerations concerning boundary conditions, z is a function of internal (plate geometry) and external (sound and flow characteristics) parameters. In the case of a perforated plate of thickness e , holes diameter d and porosity σ , z can be written as :

$$z = z(e, d, \sigma, \omega, |v|, M) \tag{5}$$

where :

ω is the sound pulsation,

$|v|$ is the amplitude of normal acoustic velocity,

M is the flow Mach number (but other characteristics of the flow are used among authors : boundary layer thickness⁴, friction velocity⁵⁻⁷).

Figure 2 resumes these considerations.

Impedance models are mainly empirical, particularly as functions of grazing flow characteristics. In order to measure impedance of layers used on Airbus aircrafts, EADS laboratory has set up a measurement bench⁸.

The aim of the present work is to compare empirical impedance models and experimental data from this bench, as functions of frequency and acoustic velocity, in order to validate experimental results. High velocity tangential air flow measurements are then presented and are compared with empirical models from literature.

Perforated plate acoustic impedance properties

This section describes perforated plates impedance properties with respect to main parameters (geometric parameters, sound frequency, acoustic velocity and flow characteristics). We chose a perforated plate to validate our results because this type of layer has been widely studied^{6,7,9-11}. Plate properties are generally deduced from the case of a single orifice.

Frequency effect : linear model

Linear model is based on acoustic propagation in a small tube representing one orifice, in a viscous fluid. Perforated plate impedance is deduced from orifice impedance writing volume velocity continuity from one hole to the whole perforated plate. Provided that :

$$|k_s d/2| > 10, \quad (6)$$

where $|k_s| = \left| \frac{-j\omega}{\nu} \right|^{1/2}$ is the Stokes wave number, characteristic of viscous effects, and ν is the kinematic viscosity of the fluid (for air, $\nu = 1.5 \cdot 10^{-5} \text{m}^2 \text{s}^{-1}$), and

$$kd/2 < \frac{1}{4}, \quad (7)$$

viscous and radiation effects in the small tube lead to the following expression for impedance of a perforated plate of thickness e , hole diameter d and porosity σ ^{9,11} :

$$z = r + j\chi \quad (8)$$

with :

$$r = \frac{\sqrt{8\nu\omega}}{\sigma c_0} \left(1 + \frac{e}{d} \right) + \frac{1}{8\sigma} (kd)^2, \quad (9)$$

and :

$$\chi = \frac{\omega}{\sigma c_0} \left[e + \frac{8d}{3\pi} (1 - 0,7\sqrt{\sigma}) + \sqrt{\frac{8\nu}{\omega}} \left(1 + \frac{e}{d} \right) \right]. \quad (10)$$

Considering frequencies of interest and geometry of the tested plates, conditions (6) and (7) are verified for the plate tested in the present work.

Acoustic velocity effect : nonlinear model

Nonlinear orifice behavior occurs when the acoustic properties of the orifice depend upon the acoustic velocity¹². This nonlinear phenomenon is explained by apparition of vorticity near orifice. Measurements show that perforated plate resistance increases with acoustic velocity ; depending on the authors, reactance decreases or stays constant.

Resistance is often written :

$$r(\omega, |v_o|) = A(\omega) + B|v_o|, \quad (11)$$

where :

$A(\omega)$ is given by expression (9),

$|v_o|$ is the incident acoustic velocity on one orifice of the plate.

Effect of frequency and velocity would thus be additive.

Factor B has different expressions depending on the authors^{9,11,13}. It is often given by¹¹ :

$$B = \frac{4}{3\pi} \frac{1 - \sigma^2}{\sigma c_0 C_D^2}, \quad (12)$$

where C_D is a discharge coefficient varying from 0.6 to 0.8.

Grazing air flow effect

Grazing air flow effect is mainly described by empirical formulas^{6,7,9,13,14}. In order to study effect of flow on a perforated plate, a lot of studies are based on the case of a single orifice placed on a rigid-walled cavity and flush mounted to a flow duct^{4,5,15,16}. Most of experimental studies and accompanying empirical models show that a grazing air flow at one hole surface increases acoustic resistance and decreases acoustic reactance.

A physical explanation of this phenomenon is given by Hersh¹⁰ : "The interaction between the grazing flow and sound-pressure field causes some of the grazing flow to be injected into the cavity over the inflow half-cycle and then ejected over the outflow half-cycle. Far from the orifice, the grazing flow is steady. [...] In both cases, the effective area through which the sound particle volume flow enters and exit the cavity appears to be less than the orifice area". Considering expressions (9) and (10), this would explain that resistance increases and reactance decreases with air flow.

Results of different studies concerning impedance variation with flow are shown on figure 3 for a perforated plate ($e = 1,02 \text{ mm}$, $d = 0,68 \text{ mm}$, $\sigma = 1,39 \%$).

Discrepancies between models can be explained by several facts. First, experimental techniques differ among authors (based on two-microphones method, Kundt tube...). Secondly, layers (or orifices) and cavity geometry leads to different physical behaviours (Helmoltz or quarter-wavelength resonators). Moreover, flow boundary layer characteristics might be different among authors. Best flow characteristic parameter seems indeed to be the friction velocity (characteristic of inner boundary layer)⁵⁻⁷. Unfortunately, some models are only based on the flow duct Mach number^{9,16}. Finally, most of the models are developed for relatively low flow velocity (about 70 m/s), not representative of the nacelle environment. It seems thus difficult to verify our set-up results using an impedance model.

Despite this fact, one empirical model has retained our attention because the experimental bench used is quite similar to ours. It has been developed by Kirby and Cummings⁷. They also tested perforated plates (porosity from 20 to 27 %, plate thickness $e = 1$ or $1,5 \text{ mm}$, orifices diameter 3 mm). Explored frequencies vary from 1000 to 7000 Hz and air flow speed reaches 70 m/s. Pressure amplitude is very low in order to neglect nonlinear effects.

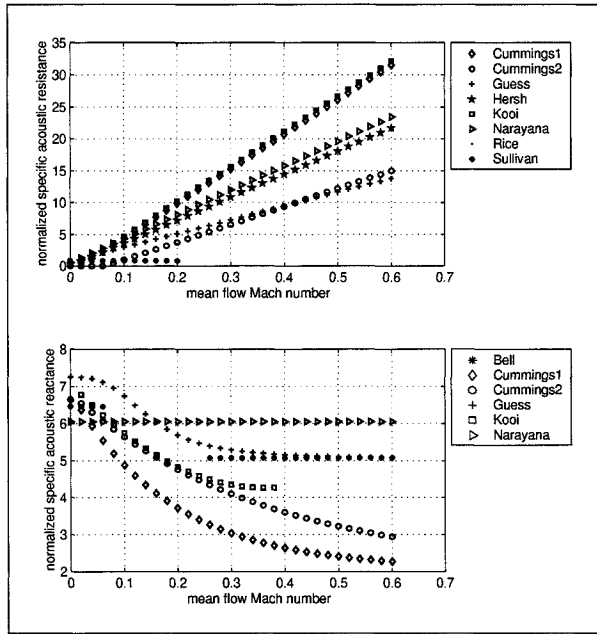


Fig. 3 Acoustic impedance of a perforated plate ($e = 1,02 \text{ mm}$, $d = 0,68 \text{ mm}$, $\sigma = 1,39 \%$) ; $f = 3150 \text{ Hz}$, $\nu = 10^{-6} \text{ m}^2/\text{s}$ as a function of Mach number ; Bell : ref.¹⁴ , Cummings1 : ref.⁷ , Cummings2 : ref.¹⁷ , Guess : ref.⁹ , Hersh : ref.¹⁸ , Narayana : ref.¹⁸ , Rice : ref.¹⁹

Following empirical formula is proposed for resistance :

$$r = \frac{\sqrt{8\nu\omega}}{\sigma c_0} \frac{e}{d} + \left[26.16 \left(\frac{e}{d} \right)^{-0.169} - 20 \right] \frac{v^*}{\sigma c_0} - 4.055 \frac{fe}{\sigma c_0} \quad (13)$$

and for reactance :

$$\chi = \frac{\omega}{\sigma c_0} \left[e + \epsilon \frac{8d}{3\pi} \right] \quad (14)$$

with :

$$\epsilon = 1 \text{ if } \frac{v^*}{fe} \geq 0.18 \frac{d}{e} \quad (15)$$

and

$$\epsilon = \left(1 + 0.6 \frac{e}{d} \right) e^{-\frac{\frac{v^*}{fe} - 0.18 \frac{d}{e}}{1.8 + \frac{d}{e}}} - 0.6 \frac{e}{d} \text{ if } \frac{v^*}{fe} > 0.18 \frac{d}{e} \quad (16)$$

In these expressions, v^* is the friction velocity, characteristic of the inner viscous boundary layer of the fluid, and seems to be the best parameter to characterize effect of flow at the surface of the resistive layer^{6,7}.

Frequency, acoustic velocity and grazing air flow effects

An interesting study has been developed by Goldman and Panton⁵. This study does not give any

impedance model but permits to define some regions of impedance behavior with respect to combined effects of frequency, acoustic velocity and flow effect by use of adimensional parameters. They measured single orifices impedance under a turbulent boundary layer. Flow velocities vary from 16 to 30 m/s, frequencies from 250 to 2500 Hz and pressure amplitude from 85 to 140 dB.

Best correlation of resistance is obtained for :

$$\frac{c_0}{\sqrt{\nu\omega}} r = F \left(\frac{e}{d}, \frac{\omega d^2}{\nu}, \frac{v^* d}{\nu}, \frac{v_o}{v^*} \right) \quad (17)$$

where F is a function of the four parameters,

and for reactance, best correlation is obtained using a term of length correction e_a :

$$e_a = \frac{\chi/(kd) - e/d}{8/(3\pi)} = F \left(\frac{e}{d}, \frac{\omega d^2}{\nu}, \frac{v^* d}{\nu}, \frac{v_o}{v^*} \right) \quad (18)$$

The different adimensional parameters allow to interpret physical phenomena :

- $\frac{\omega d^2}{\nu}$ is the square of orifice diameter over viscous diffusion,
- $\frac{v^* d}{\nu}$ is the orifice diameter over inner boundary layer length scale,
- $\frac{v_o}{v^*}$ is the ratio of acoustic momentum to boundary layer momentum.

This study shows that nonlinear resistance behavior occurs when the ratio $\frac{v_o}{v^*}$ is greater than three. Nonlinear behavior of reactance is not observed ; it would begin at higher orifice velocities than non linear resistance.

Description of the experimental set-up

This section presents the principle of measurement method and describes the experimental set-up existing at EADS laboratory. Two measurement techniques have been tested and are presented : one using a moving microphonic probe, and another using two classical 1/8" microphones.

Measurement method principle

The measurement method used at EADS laboratory is based upon the "two-microphones" technique, which was first developed by Dean²⁰. A sample of the layer under test is placed on a rigid-walled cavity, whose cross dimensions are much lower than wavelength. The set is flush mounted to a flow duct. The material is submitted to an acoustic plane wave at grazing incidence. Sound pressure is measured at two positions : one at the sample surface and one at the rear wall of the cavity. The normal acoustic velocity is assumed constant across the sample, equal to :

$$v = j \frac{p_0}{\rho_0 c_0} \sin(kL) \quad (19)$$

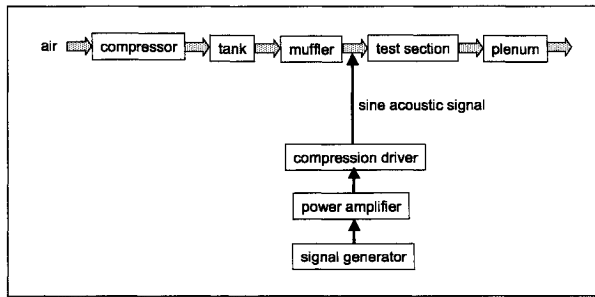


Fig. 4 Scheme of the set-up used at EADS laboratory for measuring acoustic impedance with grazing flow

where p_0 is the pressure at the rear wall of the cavity (see figure 2).

A simple calculation then gives for layer impedance :

$$z = -j \frac{1}{\sin(kL)} \frac{p}{p_0} + j \cot(kL). \quad (20)$$

For each value of frequency, acoustic velocity and Mach number, layer impedance z is then deduced from two pressure measurements (p and p_0). This method is particularly fitted for measurement of thin layers impedance with grazing flow. Other methods exist^{18,21} but they imply a complicated model of sound pressure in the duct with flow. Therefore, we preferred a “direct” method which does not need assumptions about sound pressure field in the duct.

Description of the bench

A general view of the bench is shown on figure 4. The flow is generated by a compressor, silenced by a muffler. Air flow passes through a cylindrical duct (diameter 100 mm). The sinusoidal acoustic signal is generated by a compression driver (acoustic pressure levels up to 150 dB).

The test section is a squared section rigid-walled duct (section $24 \times 24 \text{ mm}^2$) and is 860 mm long. Cut-off frequency is therefore about 7100 Hz.

A sample of the tested resistive layer ($24 \times 24 \text{ mm}^2$) is flush mounted to the duct wall, and backed by a small squared cavity specially built for measurement (24 mm side, 10 mm depth).

Aerodynamic characteristics

Pressure taps, a diaphragm and a Pitot tube allow to measure aerodynamic characteristics in the test section.

The diaphragm measures volume velocity in the 100 mm diameter duct, and gives by continuity mean velocity in the test section. Pitot tube measures maximum velocity in the test section, near the acoustic measurement region. Static pressure taps at the wall of the squared duct, allow to deduce friction velocity, which is an important parameter to study flow effects on impedance.

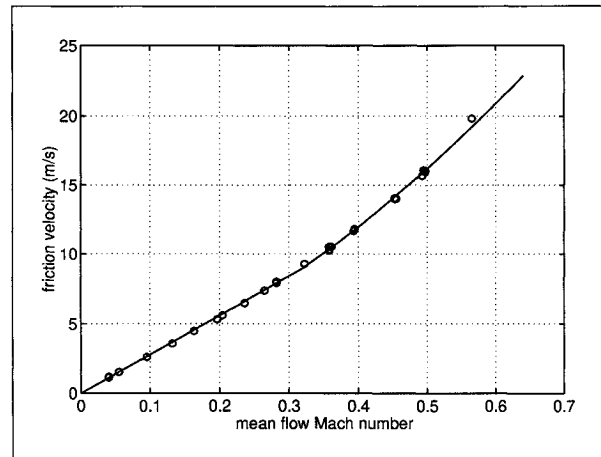


Fig. 5 Friction velocity as a function of Mach number

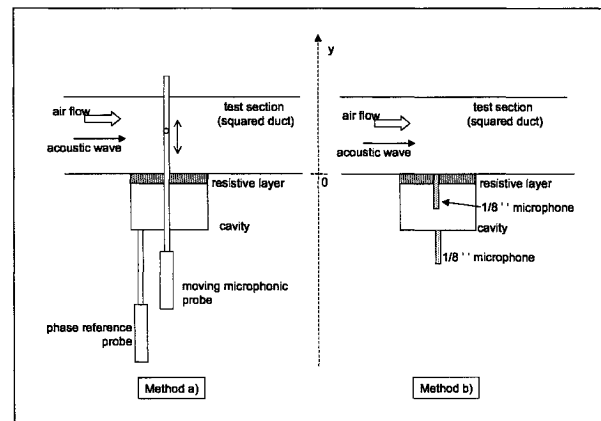


Fig. 6 Description of the measurement methods : a) method using a moving microphonic probe ; b) method using two 1/8” classical microphones

It is given by :

$$v^* = \sqrt{\frac{a}{2\rho_0} \frac{dP}{dx}}. \quad (21)$$

where a is the length of the side of the squared duct and P is the parietal static pressure. By measuring static pressure in several points at the wall of the duct, an interpolation is made to obtain the slope $\frac{dP}{dx}$ for each value of Mach number. Dependency of friction velocity with Mach number is presented on figure 5.

In the test section, flow is turbulent for the flow velocities considered (15 m/s to 240 m/s giving Reynolds numbers from 27000 to 380000). Flow velocity profile measurements showed indeed typical turbulent profiles.

Impedance measurement method using a moving microphonic probe

A microphonic probe (*Brüel & Kjaer 4182*) is placed on a motorized micrometric displacement system. The

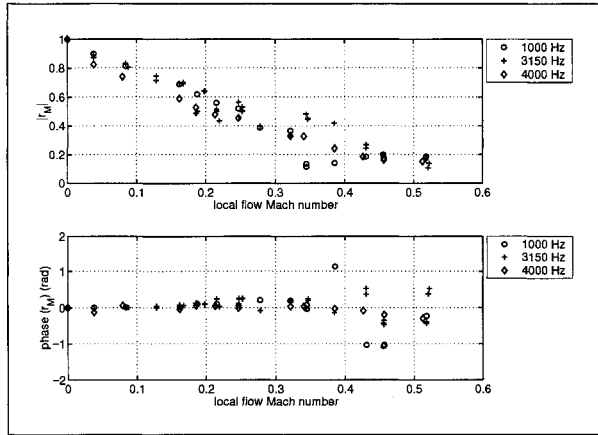


Fig. 7 Microphonic probe response as a function of Mach number for three frequencies ; probe position at $y=12$ mm

probe crosses the cavity and the duct, measuring acoustic pressure from the rear wall of the cavity to the opposite side of the duct (see figure 6a). The outer diameter of the probe (total length : 186 mm) is 1.5 mm. Two holes (diameter 0.9 mm) are drilled perpendicular to the probe axis, at 100 mm from the microphone diaphragm. The phase reference is the signal measured by another probe flush mounted at the rear of the cavity.

A difficulty of this technique is the probe calibration with flow. Indeed, probe holes impedance vary with Mach number. An experimental method has been set-up in order to measure probe response with flow⁸, based on Chung and Blaser technique²².

Measured probe response as a function of local Mach number (Mach number at the probe position) is given on figure 7. Probe has been first calibrated with respect to frequency. This figure shows that probe sensitivity decreases very much with increasing flow velocity and that phase measurements are very scattered.

A correction function r_M has been deduced from these measurements to take into account this change in sensitivity :

$$r_M(f, y) = e^{-\alpha(f)M(y)}, \quad (22)$$

where :

$\alpha(f)$ is a parameter determined empirically from probe calibration measurement, depending on frequency,

$M(y)$ is the local flow Mach number depending on the section probe position (y axis).

Following expression (20), layer impedance is then given from probe measurements by :

$$z = -j \frac{p(y_s) r_M(f, y_r)}{p(y_r) r_M(f, y_s)} \frac{1}{\sin(kL)} + j \cot(kL), \quad (23)$$

where :

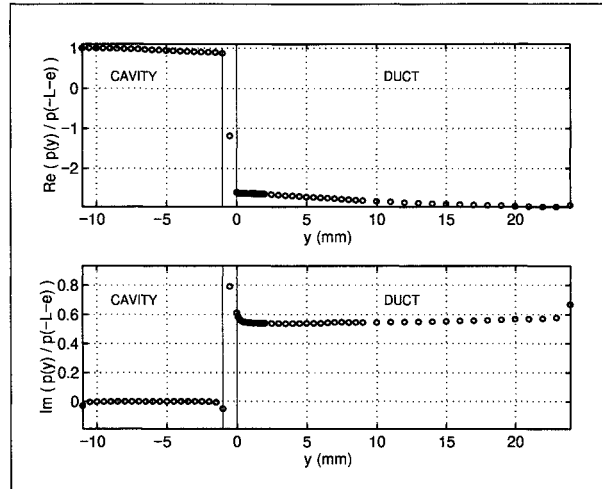


Fig. 8 Example of pressure profile measured by moving microphonic probe ; vertical lines symbolises layer position ; $y = -L - e$ corresponds to the rear wall of the cavity and $y = 0$ corresponds to layer surface

$p(y_s)$ is the pressure measured at the layer surface,

$p(y_r)$ is the pressure measured at the rear of the cavity.

An example of pressure profile is given on figure 8. Theoretically, y_r and y_s should be at exact positions. In practice, measurement region being not a dot (the probe holes diameter is 0.9 mm), points y_s and y_r are chosen by the experimenter to deduce impedance. Point y_r is chosen at the rear of the cavity so that pressure amplitude is maximum ; point y_s is chosen near layer surface, but not too close in order to avoid a measure of pressure in the near field of the layer.

From these measurements, standing wave pattern in the cavity is verified (of the form $\cos(ky)$) and pressure field in the duct is also known. Pressure profile in the duct is not exactly uniform, due to impedance change between the rigid wall of the the duct and the layer sample.

Figure 9 presents several pressure profiles for different Mach numbers. It can be observed that pressure jump across the layer varies with flow velocity, showing already influence of flow on layer impedance. Near the layer ($0 < y < 2$ mm), the flows induces a strong pressure gradient, particularly on imaginary part. Therefore, impedance deduction, which is linked to the choice of a measurement point near layer surface, will be delicate.

This method thus allows to measure pressure field at any point in the duct section but difficulties come from probe calibration with flow and choice of a measurement point at the layer surface.

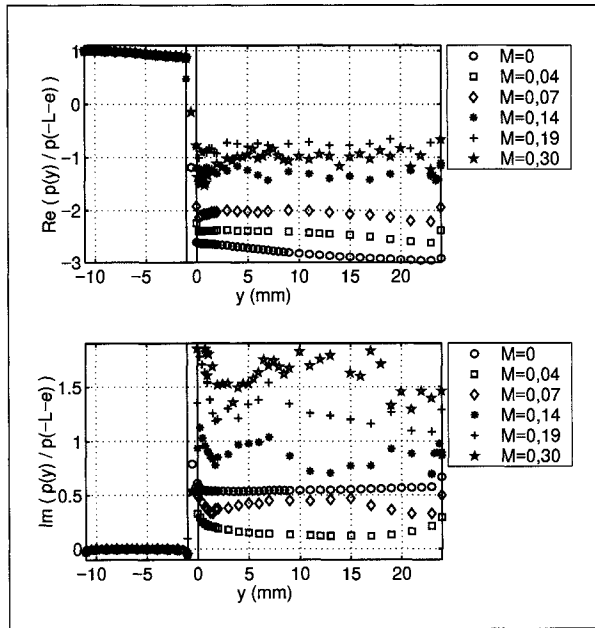


Fig. 9 Pressure profiles measured by moving microphonic probe at different mean flow Mach numbers on a perforated plate ($e = 1,02 \text{ mm}$, $d = 0,68 \text{ mm}$, $\sigma = 1,39 \%$); vertical lines symbolises layer position ; $f=3150 \text{ Hz}$, $|v|=0.025 \text{ m/s}$

Impedance measurement method using two 1/8” microphones

Probe calibration difficulty and measurement disturbance (due to the fact that probe crosses the duct section) has lead to perform another measurement technique, using two 1/8” classical microphones (*Brüel & Kjør 4138*). One microphone is flush mounted at the surface of the layer ; another is flush mounted at the rear of the cavity (see figure 6b).

This technique implies to calibrate the two microphones. Both of them are placed at the rear of the cavity, where pressure field is uniform. By measuring transfer function between the microphones, they are calibrated one in comparison with the other. The corrective transfer function is presented on figure 10.

Impedance is then given by :

$$z = -j \frac{H}{H_c} \frac{1}{\sin(kL)} + j \cot(kL), \quad (24)$$

where H is the measured transfer function between microphones and H_c is the corrective transfer function.

An advantage of this method is that it is non intrusive and that microphones response is independant of flow velocity. However, these very small microphones (3.2 mm diameter) are little sensitive (about 0.8 mV/Pa) and very fragile.

Experimental results

In order to validate measurements results, they were first compared in the case of zero mean flow with

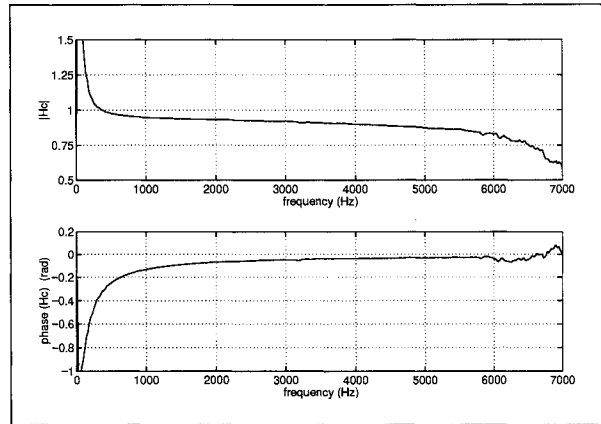


Fig. 10 Corrective transfer function between 1/8” microphones

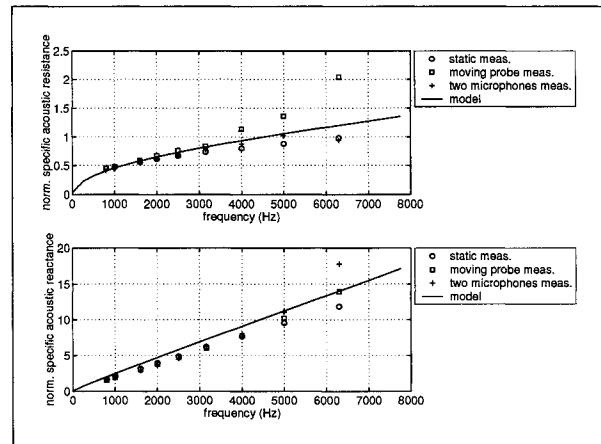


Fig. 11 Comparison between impedance measurement results from : flow duct (using moving probe or two microphones), static bench and linear model (expressions (9) and (10)), for a perforated plate ($e = 1,02 \text{ mm}$, $d = 0,68 \text{ mm}$, $\sigma = 1,39 \%$) ; $|v|=0.001 \text{ m/s}$, $M=0$

impedance models as a function of frequency and acoustic velocity. Measurements with grazing flow were then performed.

Impedance measurements with respect to frequency

Figure 11 shows measurements on a perforated plate as a function of sound frequency, at zero mean flow and at very low acoustic velocity in order to neglect nonlinear effects.

The graph also shows results from another experimental set-up existing at EADS laboratory. It is a “static bench” (no-flow duct) measuring acoustic impedance with a moving microphonic probe (same deduction method as in the flow duct). A major difference with the air flow set-up is that acoustic wave incidence is normal to the layer surface (in the flow duct, wave is at grazing incidence).

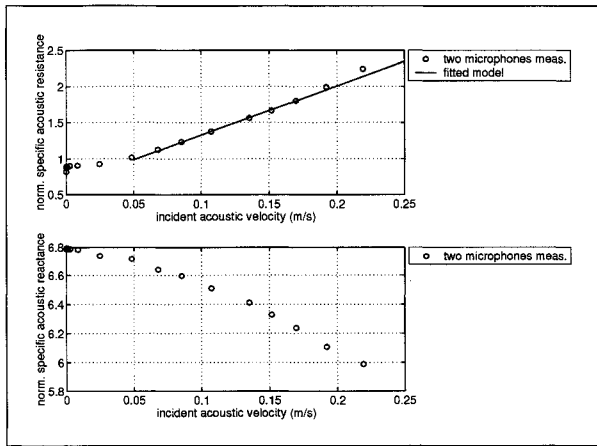


Fig. 12 Impedance measurements with respect to acoustic velocity for a perforated plate ($e = 1,02$ mm, $d = 0,68$ mm, $\sigma = 1,39$ %) ; $f=3150$ Hz, $M=0$

Good comparison is observed between two-microphones measurements, static bench results and linear model (expressions (9) and (10)). Perforated plate impedance would then not vary with incidence. Moving probe resistance measurements do not agree quite well with others results, over 4000 Hz, which has not been explained up to now.

Impedance measurements with respect to acoustic velocity

The same perforated plate has been tested with respect to acoustic velocity, using the two microphones. Expected tendencies arise (increasing of resistance and decreasing of reactance). Expression (11) fits the experimental data for $|v| > 0.05$ m/s, taking $C_D=1$ in expression (12) of factor B . For the low velocities region ($|v| < 0.05$ m/s), a parabolic shape of resistance is observed, as expected from the work of Aurégan and Pachebat²³.

Impedance measurements with respect to grazing air flow velocity

Measurement results with grazing flow are presented on figure 13. It can be seen that two microphones results fit best with empirical formula from Kirby and Cummings (see expressions (13) and (14)). They also used classical microphones in a flow duct. Their formula has been developed up to Mach 0.2. It is shown that it can be extended to Mach 0.6. Perforated plate impedance properties would then not be modified at “low” ($M < 0.2$) and “high” Mach numbers ($M > 0.2$).

Measurements results from moving probe do not agree very well with other results. We suppose that it is due to errors in the probe calibration. Moreover, with the probe, pressure is measured *near* the layer surface, somewhere in the boundary layer. With microphones, pressure is measured *at* the layer sur-

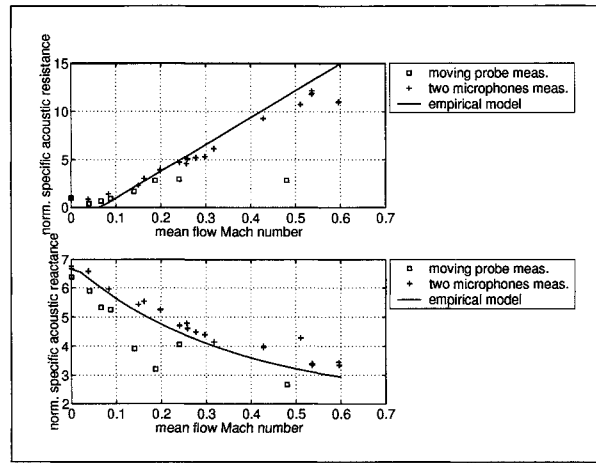


Fig. 13 Impedance measurement on a perforated plate ($e = 1,02$ mm, $d = 0,68$ mm, $\sigma = 1,39$ %) with respect to mean flow Mach number ; $f=3150$ Hz ; $|v|=0.025$ m/s ; empirical model : see expressions (13) and (14)

face. Therefore, deduced impedances could not have the same properties in the two cases.

Acoustic velocity and grazing air flow effects

Cumulative effects of flow and acoustic velocity are presented on figure 14. We used dimensional analysis of Goldman (see expressions (17) and (18)). Measurements are performed with the two 1/8” microphones, for three Mach numbers, at different acoustic velocities.

For $M = 0.15$, two different behaviors of resistance are observed around $\frac{v_a}{v} = 1$. When $\frac{v_a}{v} < 1$, resistance is practically constant and then increases for $\frac{v_a}{v} > 1$. Goldman’s measurement, at Mach 0.1, give a limit of 3. It is shown that limit value of $\frac{v_a}{v}$ diminishes when Mach number increases (0.3 for Mach 0.30 and 0.1 for Mach 0.51). Nonlinear behaviour would then appear more “quickly” at high Mach number. It is also shown a slight decreasing of resistance for $0.4 < \frac{v_a}{v} < 1$ at Mach 0.15. Goldman indicates that this behavior can be observed when the parameter $\frac{v_a^* d}{\nu}$ is lower than 250 ; in our case it is equal to 190 which shows agreement with Goldman result. For $M = 0.30$ and $M = 0.51$ this behavior is not observed as expected ($\frac{v_a^* d}{\nu}$ is then higher than 250).

Conclusion

The aim of this paper was to present a method of measuring acoustic impedance of thin layers with grazing air flow. Two measurement techniques have been studied, one using a moving microphonic probe and another using two 1/8” classical microphones. It is shown that the second method is easier to use and give better results by comparison with models from literature. However, moving probe method should not be given up because it gives more informations (pres-

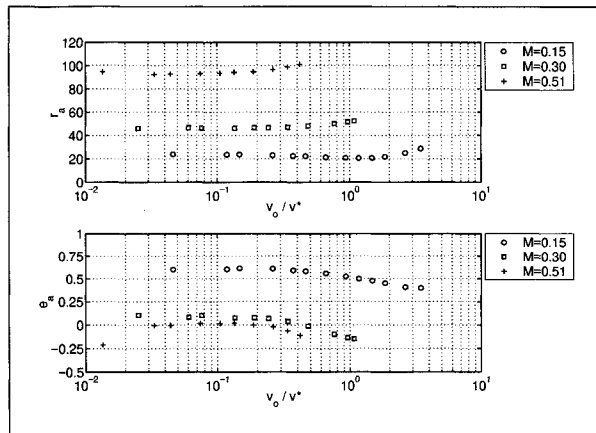


Fig. 14 Acoustic velocity and grazing air flow effects on perforated plate impedance ($e = 1,02 \text{ mm}$, $d = 0,68 \text{ mm}$, $\sigma = 1,39 \%$) ; $f=3150 \text{ Hz}$; r_a : see expression (17) ; e_a : see expression (18)

sure field being measured at numerous points across the duct).

The tested layer is a perforated plate, this type of material being widely studied.

By comparison with an empirical formula from literature, it has been shown that our bench gives reasonably good results. Moreover, this formula has been developed for a maximum Mach number of 0.2. Present results show that it can be extended to Mach 0.6. Perforated plate impedance would then not be modified at low or high Mach number.

Measurements on other types of layers (perforated plate with different geometries, wire-mesh) are now being studied.

References

- ¹Montétagaud, F., *Modélisation de la propagation et du rayonnement acoustiques des entrées d'air de turboréacteurs*, Ph.D. thesis, Université du Maine, Le Mans, 1998.
- ²Aurégan, Y., Starobinski, R., and Pagneux, V., "Influence of grazing flow and dissipation effects on the acoustic boundary conditions at a lined wall," *J. Acoust. Soc. Am.*, Vol. 109, No. 1, 2001, pp. 59–64.
- ³Zorumski, W. and Tester, B., "Prediction of the acoustic impedance of duct liners," *NASA Technical Memorandum*, Vol. 79951, 1976.
- ⁴Ronneberger, D., "The acoustical impedance of holes in the wall of flow ducts," *J. Sound Vib.*, Vol. 24, No. 1, 1972, pp. 133–150.
- ⁵Goldman, A. and Pantan, R., "Measurement of the acoustic impedance of an orifice under a turbulent boundary layer," *J. Acoust. Soc. Am.*, Vol. 60, No. 6, 1976, pp. 1397–1404.
- ⁶Kooi, J. and Sarin, S., "An experimental study of the acoustic impedance of Helmholtz resonator arrays under a turbulent boundary layer," *AIAA 7th Aeroacoustics Conference*, No. AIAA-81-1998, 1981.
- ⁷Kirby, R. and Cummings, A., "The impedance of perforated plates subjected to grazing gas flow and backed by porous media," *J. Sound Vib.*, Vol. 217, No. 4, 1998, pp. 619–636.
- ⁸Malmary, C., *Etude théorique et expérimentale de l'impédance acoustique de matériaux en présence d'écoulement*

d'air tangentiel, Ph.D. thesis, Université du Maine, Le Mans, 2000.

⁹Guess, A., "Calculation of perforated plate liners parameters from specified acoustic resistance and reactance," *J. Sound Vib.*, Vol. 40, No. 1, 1975, pp. 119–137.

¹⁰Hersh, A. and Walker, B., "Acoustic behavior of Helmholtz resonators: part II. Effects of grazing flow," *CEAS/AIAA*, Vol. CEAS/AIAA-95-079, 1995.

¹¹Melling, T., "The acoustic impedance of perforates at medium and high sound pressure level," *J. Sound Vib.*, Vol. 29, No. 1, 1973, pp. 1–65.

¹²Pantan, R. and Goldman, A., "Correlation of nonlinear orifice impedance," *J. Acoust. Soc. Am.*, Vol. 60, No. 6, 1976, pp. 1390–1396.

¹³Sullivan, J., "A method for modeling perforated tube muffler components. I. Theory," *J. Acoust. Soc. Am.*, Vol. 66, No. 3, 1979, pp. 772–778.

¹⁴Bell, W., Daniel, B., and Zinn, B., "Acoustic liner performance in the presence of a mean flow and three-dimensional wave motion," *AIAA 12th Aerospace Sciences Meeting*, No. AIAA-74-61, 1974.

¹⁵Cummings, A., "The response of a resonator under a turbulent boundary layer to a high amplitude non-harmonic sound field," *J. Sound Vib.*, Vol. 115, No. 2, 1987, pp. 312–328.

¹⁶Hersh, A. and Walker, B., "Effect of grazing flow on the acoustic impedance of Helmholtz resonators consisting of single and clustered orifices," *NASA Contractor Report*, Vol. 3177, 1979.

¹⁷Cummings, A., "The effects of grazing turbulent pipe-flow on the impedance of an orifice," *Acustica*, Vol. 61, 1986, pp. 233–242.

¹⁸Narayana Rao, K. and Munjal, M., "Experimental evaluation of impedance of perforates with grazing flow," *J. Sound Vib.*, Vol. 108, No. 2, 1986, pp. 283–295.

¹⁹Rice, E., "A theoretical study of the acoustic impedance of orifices in the presence of a steady grazing flow," *NASA Technical Memorandum*, Vol. 71903, 1976.

²⁰Dean, P., "An in-situ method of wall acoustic impedance measurement in flow ducts," *J. Sound Vib.*, Vol. 34, No. 1, 1974, pp. 97–130.

²¹Watson, W., Jones, M., and Parrott, T., "Validation of an impedance education method in flow," *AIAA*, Vol. AIAA-98-2279, 1998.

²²Chung, J. and Blaser, D., "Transfer function method of measuring in-duct acoustic properties. I. Theory," *J. Acoust. Soc. Am.*, Vol. 68, No. 3, 1980, pp. 907–913.

²³Aurégan, Y. and Pachebat, M., "Measurement of the nonlinear behavior of acoustical rigid porous materials," *Physics of Fluid*, Vol. 11, No. 6, 1999, pp. 1342–1345.